BAU Journal - Science and Technology

Manuscript 1107

OPTIMIZATION OF THE BIO-SYNTHESIS OF MAGNESIUM NANOPARTICLES FROM STAPHYLOCOCCUS HAEMOLYTICUS: A PILOT STUDY

Mariam Bassam

Malak Mezher

Mahmoud khalil

1. INTRODUCTION

Thoughts on nanoscience first surfaced in 1959 by Richard Feynman. However, Professor Norio Taniguchi was the first to use the term "Nanotechnology" about a decade later. Since then, researchers have been examining overlooked aspects of nanotechnology with great interest. Thus, the use of nanotechnology has dramatically expedited research and caused the development of innovative skills in multidisciplinary scientific fields (Bayda et al., 2019).

Nanotechnology is the study of manipulating and controlling materials made of single atoms or molecules. It focuses on the nanoscale level, which can handle materials ranging from 1 to 100 nanometers (nm). Furthermore, nanotechnology gives rise to two distinct types of nanomaterials: natural ones found in nature and artificial ones that are synthetically made. These materials have a significantly larger surface area, facilitating more significant interaction between atoms and other matter. Consequently, nanomaterials exhibit superior durability and conductivity compared to more extensive materials. Additionally, their large surface area, surface energy, and quantum confinement are attributed to their various properties, including optical, mechanical, physical, and chemical properties (luids et al., 2021).

NPs are a pivotal product of nanotechnology, which finds applications in various fields such as medicine, cosmetics, and electronics (luids et al., 2021). The minute size of these materials plays a crucial role in determining their properties and activities on a nanometer scale, as atoms reflect light differently. With a complex structure, NPs usually comprise three layers: the surface layer, the shell layer, and the core. Scientists worldwide are exploring this exceptional material's endless possibilities (Roco et al., 2012).

Nonetheless, traditional synthesis methods include physical, chemical, and biological. Physical methods for synthesizing NPs could be more efficient, requiring significant time and energy (“The different dimensions of nanotechnology,” 2009). Chemical methods also present a disadvantage as they involve toxic and harsh chemicals. However, some chemical methods, especially the co-precipitation method, are before others due to the low cost and the easy use of pH in the synthesis process (Adnan et al., 2023). For this reason, the bio-synthesis of NPs is preferred and involves using microorganisms and plants, even though it is slow with other cons (Singh et al., 2020).

Green nanotechnology has become a favored alternative to the biological methods of synthesizing NPs (Singh et al., 2020; Uddin et al., 2021; Younis et al., 2021). This eco-friendly and cost-effective method has gained significant importance recently due to its simplicity and effectiveness in generating NPs through biotechnological techniques (Nicolae-Maranciuc et al., 2022). Many NPs synthesized through green nanotechnology have been proven efficient in various applications (Hamida et al., 2023). The biological approaches are economical and harmless. They use ecologically compatible solvents made of stabilizing and reducing agents (Younis et al., 2021).

The use of metallic-based nanoparticles has become increasingly popular in biological techniques. Typical metals used include zinc, copper, silver, iron, and gold, as they possess unique physical and chemical properties with a wide range of applications in the biological field (Adnan et al., 2023; Devi etal., 2017; Uddin et al., 2021; Younis et al., 2021; Zia et al., 2017). One metal that stands out for being safe and non-toxic is magnesium (Mg). Mg nanoparticles are highly effective as antimicrobial agents and have unique bio-compatible properties. They are efficient and can withstand high activity, making them advantageous (Adnan et al., 2023; Adnan et al., 2023; Younis et al., 2021).

Certain bacteria effectively produce NPs through bio-synthesis. Previous research has demonstrated the efficient creation of silver NPs by bacteria such as *P. aeruginosa*, *E. coli*, and *K. pneumoniae* (Dolati et al., 2023; Saleh et al., 2020). Magnesium NPs, on the other hand, are typically synthesized by plants rather than bacteria (Younis et al., 2021). Interestingly, there is no record of bacterial synthesis of Mg NPs in previous literature. While *P. aeruginosa* and *K. pneumoniae* are used for synthesizing NPs, especially silver NPs. Most studies have focused on Gram-negative bacteria (Devanesan et al., 2021; Devi et al., 2017; Feroze et al., 2020; Rahman et al., 2019; Sudarsan et al., 2021), however, Gram-positive bacteria also have unique properties that make them capable of producing secondary metabolites, which are effective in

synthesizing NPs (Tortorella et al., 2018). Among Gram-positive bacteria, *S. haemolyticus* is a non-motile and facultative anaerobe. It is part of the human skin flora (Barros et al., 2012).

Mg NPs has been previously bio-synthesized from plant extracts. However, bacterial synthesis of Mg NPs has not been much taken into consideration. In addition, previous research has never focused on *S. haemolyticus* as a precursor for the synthesis of metallic NPs. In this regard, this study aims to create Mg NPs using the secondary metabolites of *S. haemolyticus* found in Lebanese wastewater. The study will explore factors that can affect the synthesis process, including the concentration of bacteria used, the temperature, the concentration of Mg, and the incubation time of the bacterial metabolites with the Mg solution.

2. MATERIALS AND METHODS

2.1. Isolation of Bacteria

The bacterium (*S. haemolyticus*) was isolated from wastewater samples collected from South Lebanon Water Establishment (SLWE) in Saida. This station receives wastewater from about 70 villages in South Lebanon. *S. haemolyticus* was isolated from wastewater by spreading 100 µL of the water samples on Mannitol Salt Agar (MSA) (99 %, Sigma, 3050 Spruce Street Saint Louis, Missouri 63103 USA) and incubating them for 24 h at 37 ˚C. After incubation, the obtained bacterial colonies were Gram-stained and further identified by VITEK (VITEK 2 Automated Systems, BioMerieux Inc., Massacusetts, United States) assay (Mezher et al., 2022).

2.2. Preparation of the Bacterial Culture

A colony of *S. haemolyticus*, previously cultured on a nutrient agar (NA) (99 %, Sigma, 3050 Spruce Street Saint Louis, Missouri 63103 USA) plate, was suspended in nutrient broth (NB) (99 %, Sigma, 3050 Spruce Street Saint Louis, Missouri 63103 USA) to reach the standard turbidity (0.5 McFarland). The suspensions were incubated at 37 ˚C for 24 h.

2.3. Preparation of the Bacterial Metabolites

Following incubation, the suspensions were centrifuged at 6000 rpm for 20 min at room temperature to separate the metabolites from the bacterial cells. After centrifugation, the cells were discarded. The supernatant (containing the metabolites) was stored at 4 ˚C for synthesizing the Mg NPs (Dolati et al., 2023).

2.4. Preparation of the Mg Solutions

A specific mass of Mg nitrate (99%, Perth, Australia) was mixed with sterile distilled water to form solutions of a volume 90 mL and concentrations 1, 2, 3, 4, and 5 mM (Saleh et al., 2020). A mass of 14.83 mg of Mg nitrate was added to prepare the 1 mM solution, 29.66 mg was added to the 2 mM solution, 44.49 mg was added to the 3 mM solution, 59.32 mg was added to the 4 mM solution, and 74.15 mg was added to the 5 mM solution.

2.5. Synthesis of the Mg NPs

To create a 100 mL solution, 10 mL of prepared metabolites were added to 90 mL of Mg nitrate solution. The solutions were then incubated in a shaker incubator (Global Scientific Company, Tamil Nadu, India) under dark condition to prevent metal ion oxidation. The incubation was carried out at different temperatures (37 and 60 ˚C) and for various periods (6, 24, 48, and 72 h) while agitated at 120 rpm. The formation of NPs was confirmed by a color change from transparent to white. Negative controls were created using Mg nitrate solution mixed with NB but without bacterial metabolites. To separate the NPs, the solutions were centrifuged at 13000 rpm for 15 minutes. The resulting pellets were washed thrice with sterile distilled water and then oven-dried at 40˚C for 24 hours. The weight of the dry pellets (NPs) was measured and stored for further characterization (Dolati et al., 2023).

2.6. Characterization of the Mg NPs

To analyze the Mg NPs, we used an ultraviolet-visible spectrophotometer (UV-Vis) (UV1801 UV Vis spectrophotometer (single beam 190 – 1100 nm), Shanghai, China) that measures the color of the mixture within a range of 200 - 700 nm. This technique detects changes in the Mg NPs by measuring their ability to absorb light in the visible region. 500 µL of the Mg NPs were mixed with sterile distilled water and measured the absorbance within the mentioned range (Dolati et al., 2023; Saleh et al., 2020). In addition, the functional groups present were detected by Fourier Transform infrared spectroscopy (FTIR). The FTIR was performed at room temperature in the range 4000 – 400 cm^{-1}.

2.7. Effect of Some Physico-chemical Conditions

Different parameters were tested to determine the best conditions to produce the highest yield of the Mg NPs. The parameters included: the concentration of metal nitrate solutions, the concentration of bacteria, temperature, and time of the shaking incubation.

2.7.1 Effect of the Concentration of Mg Nitrate Solutions

The pilot experiment was designed by examining 5 different concentrations of Mg nitrate (1, 2, 3, 4, and 5 mM) to determine the optimal concentration to obtain the best yield of the synthesized NPs. The optimal concentration was detected by the change in the intensity of color and characterized by UV-Vis (Saleh et al., 2020).

2.7.2. Effect of the Concentration of Bacteria

To conduct this experiment, we examined three different concentrations of an incubated bacterial culture: 10^4 (less than 0.5 McFarland), 10^8 (0.5 McFarland), and 10^{12} (greater than 0.5 McFarland) CFU/mL. A colony of *S. haemolyticus*, previously cultured on nutrient agar, was suspended in NB and adjusted the concentration by measuring the absorbance at 600 nm. For the concentration 10^4 CFU/mL, the O.D. was below 0.08. For the concentration 10^8 CFU/mL, the O.D. was between 0.08 and 0.1, and for the concentration 10^{12} CFU/mL, the O.D. was above 0.1.

2.7.3. Effect of the Time of Incubation of the Bacterial Metabolites with the Mg Nitrate Solutions

The pilot study was designed by incubating the metabolites - Mg nitrate solutions in the shaker incubator at 120 rpm at 4 different time intervals (6, 24, 48, and 72 h). The optimum time was determined by the change in the intensity of the color and the peak of absorbance obtained by UV-Vis.

2.7.4. Effect of Temperature

The experiment was performed by incubating the solutions at 2 different temperatures (37 and 60 ˚C) to detect the optimal temperature for the synthesis of the Mg NPs. The best temperature was detected by the intensity of color and by UV-Vis (Saleh et al., 2020).

3. RESULTS

3.1. Visual Examination

After incubation of the bacterial metabolites – Mg nitrate solutions in dark conditions, the reduction happened and was observed by a color change from transparent to white, indicating the probable formation of the Mg NPs. For the negative controls, no change in color was observed. The results are presented in Figure 1.

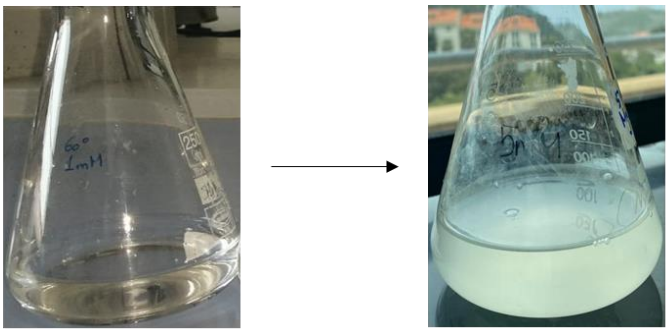

Fig.1: Change of the solution's color from transparent to white after incubation of the bacterial metabolites with the Mg nitrate solution.

3.2. Effect of the Concentration of Mg Nitrate Solutions

The Mg nitrate solutions were prepared with different concentrations (1, 2, 3, 4, and 5 mM). The significant effect was illustrated by color alteration from transparent to white and the plasmon absorbance peaks. The highest yield was recorded for the Mg nitrate solution of concentration 3 mM (Table 3). This means that the optimum concentration of Mg nitrate solution used in the synthesis of Mg NPs from *S. haemolyticus* is 3 mM. The obtained results were confirmed by the UV-Vis. The highest absorbance was recorded for the NPs prepared from 3 mM solutions with an absorbance of 0.9 a.u. within the range of 250 – 300 nm, indicating the reduction of Mg nitrates to Mg NPs (Figure 5).

3.3. Effect of the Time of Incubation of the Samples in the Shaker

The time of incubation is a biological factor that has a significant effect on the synthesis of NPs. The best time observed was 48 h (Table 3). After incubating the samples at different time intervals (6, 24, 48, and 72 h) (Tables 1, 2, and 4) and synthesizing the NPs, the highest yield was recorded for samples incubated for 48 h. These results were also confirmed by the UV-Vis spectra in which the highest peaks within the range (200 - 700 nm) were recorded for the samples incubated for 48 h, indicating the increase in the reduction of the Mg nitrate to Mg NPs (Figure 5).

3.4. Effect of Bacterial Concentration

After fixing the time parameter at 48 h (optimal timing for NPs synthesis), the bacterial concentration was adjusted to low (10^4 CFU/mL), standard (10^8 CFU/mL), and high (10^{12} CFU/mL). The best bacterial concentration was the standard (0.5 McFarland). It produced the highest yield and spectra peaks of the NPs especially at 3 mM of Mg nitrate solution (Table 3 and Figures 3, 4, 5, and 6).

3.5. Effect of Temperature

The optimum temperature for the Mg NPs synthesis was 37 ˚C (Figures 3, 4, 5, 6, 7, and 8). However, at 60 ˚C and after 48 and 72 h of incubation, no change in the color of the mixtures was observed (remained transparent) (Figure 2), indicating that the Mg nitrates weren't reduced to Mg NPs.

3.6. UV-Vis Results

The UV-Vis spectra of the synthesized Mg NPs were tested in the range 200 – 700 nm. The noticeable peaks appeared at 250 – 300 nm. The highest absorbance peaks were obtained for the samples incubated for 48 h at 37 ˚C with Mg concentration of 3 mM (Figure 5). However, the lowest peaks were observed for solutions with the Mg nitrate concentration of 2 mM incubated for 6 h at 37 ˚C (Figure 1). In addition, at low bacterial concentrations, low absorbance peaks were obtained especially for Mg nitrate concentration of 2 mM

(Figure 7). A better yield was observed for samples of higher bacterial concentration (> 10^{12} CFU/mL) (Figure 8).

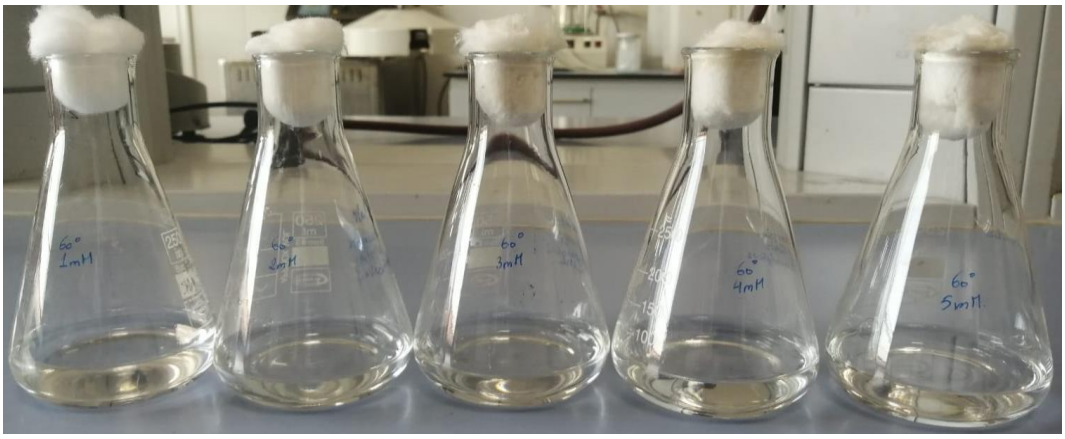

Fig.2: Results showing no reduction of Mg nitrate to Mg NPs after incubation for 48 and 72 h at 60˚C.

Collectively, the best conditions for the synthesis of Mg NPs from the metabolites of *S. haemolyticus* include Mg nitrate solution of concentration 3mM, the bacterial concentration of 10^8 CFU/mL (0.5 McFarland), temperature 37 ˚C, and shaking incubation time of 48 h.

Table 1. Masses of the obtained Mg NPs at 37 ˚C after 6 h of incubation in the shaker at 120 rpm.

Experimental conditions		Mg nitrate (mM)				
		1	2	3	4	5
		Nanoparticles (mg)				
Concentration of *S. haemolyticus* (CFU/mL)	108 (0.5 McFarland)	1.2	0.7	1.3	0.8	2.3
Temperature	37 ˚C					
Time of shaking incubation	6 h					

mM: mg/mL, CFU: colony forming unit, Mg: magnesium, NPs: nanoparticles.

Table 2 Masses of the obtained Mg NPs at 37 ˚C after 24 h of incubation in the shaker at 120 rpm.

Experimental conditions		Mg nitrate (mM)				
		1	2	3	4	5
		Nanoparticles (mg)				
Concentration of *S. haemolyticus* (CFU/mL)	10^8 (0.5 McFarland)	5.9	3.3	5.2	2.9	2.6
Temperature	37 ˚C					
Time of shaking incubation	24 h					

mM: mg/mL, CFU: colony forming unit, Mg: magnesium, NPs: nanoparticles.

Table 3 Masses of the obtained Mg NPs at 37 ˚C after 48 h of incubation in the shaker at 120 rpm.

Conditions at 37 ˚C and 48 h of shaking incubation		Mg nitrate (mM)				
		1	2	3	4	5
		Nanoparticles (mg)				
Concentration of *S. haemolyticus* (CFU/mL)	10^4 (< 0.5 McFarland)	3.6	2.2	5.7	2.2	3
	10^8 (0.5 McFarland)	9.6	9.8	10.6	10.5	10.4
	10^{12} (> 0.5 McFarland)	4	3.8	3.3	5.7	2

mM: mg/mL, CFU: colony forming unit, Mg: magnesium, NPs: nanoparticles.

Table 4 Masses of the obtained Mg NPs at 37 ˚C after 72 h of incubation in the shaker at 120 rpm.

Conditions		Concentration of Mg nitrate (mM) and mass of NPs (mg)				
		1	2	3	4	5
		Nanoparticles (mg)				
Concentration of *S. haemolyticus* (CFU/mL)	10^8 (0.5 McFarland)	5.4	6.5	1.1	3.9	7.7
Temperature	37 ˚C					
Time of shaking incubation	72 h					

mM: mg/mL, CFU: colony forming unit, Mg: magnesium, NPs: nanoparticles.

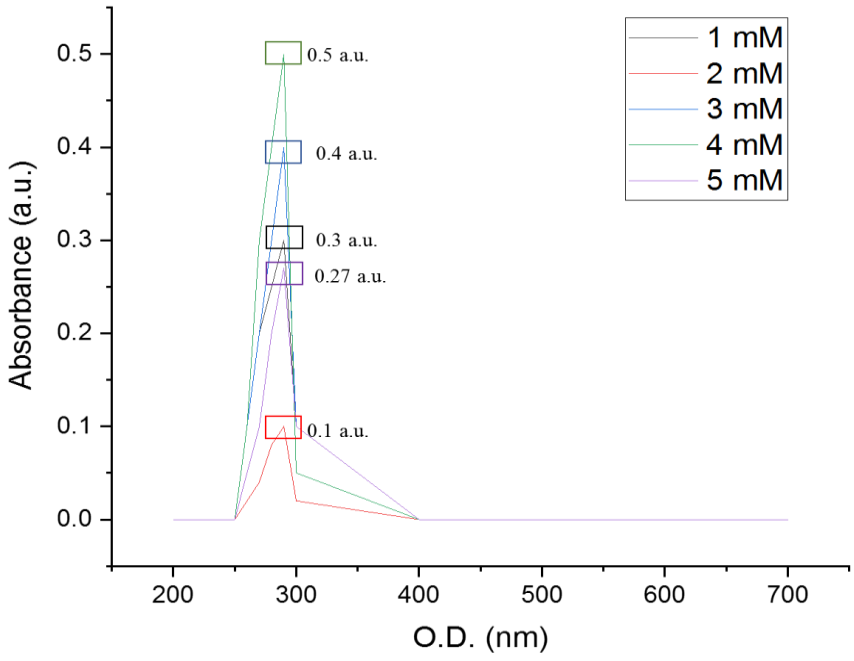

Fig.3: Absorbance peaks of the Mg NPs in the range of 200 - 700 nm synthesized under the following conditions: Temperature 37 ˚C, bacterial concentration 10^8 CFU/mL (0.5 McFarland), and time of incubation 6 h.

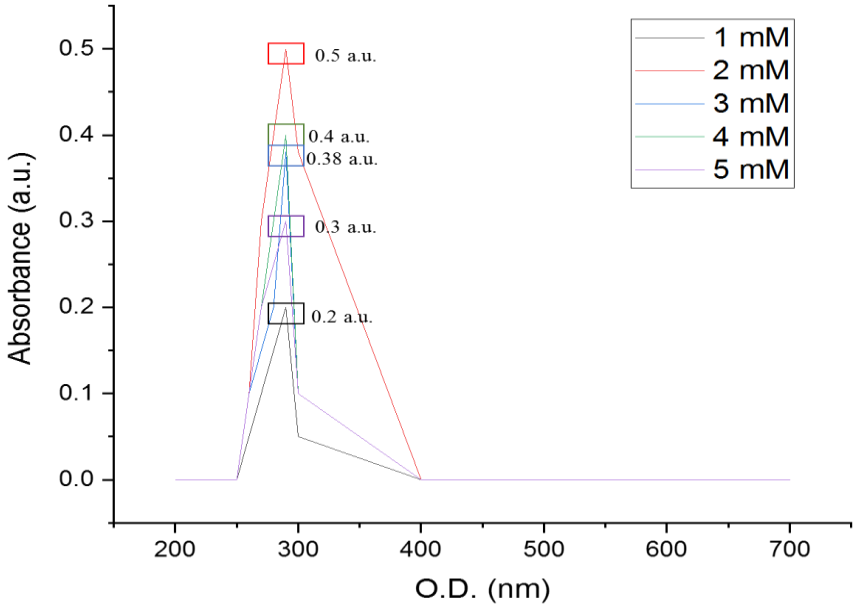

Fig.4: Absorbance peaks of the Mg NPs in the range of 200 - 700 nm synthesized under the following conditions: Temperature 37 ˚C, bacterial concentration 108 CFU/mL (0.5 McFarland), and time of incubation 24 h.

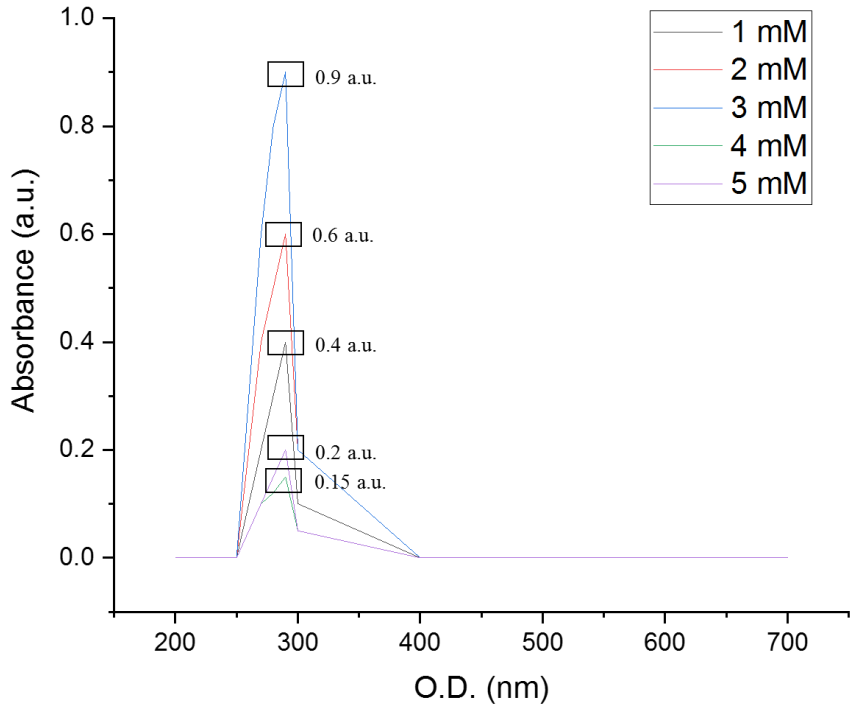

Fig.5: Absorbance peaks of the Mg NPs in the range of 200 - 700 nm synthesized under the following conditions: Temperature 37 ˚C, bacterial concentration 108 CFU/mL (0.5 McFarland), and time of incubation 48 h.

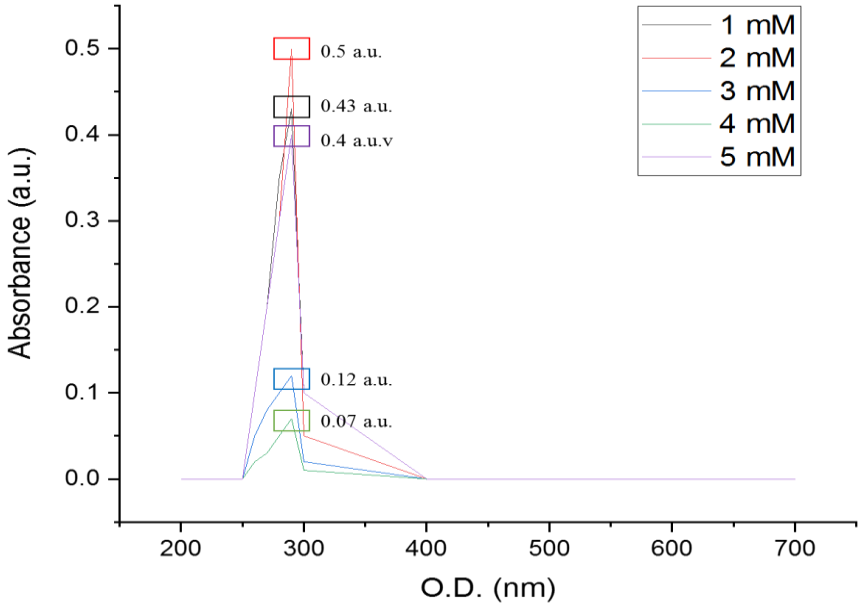

Fig.6: Absorbance peaks of the Mg NPs in the range of 200 - 700 nm synthesized under the following conditions: Temperature 37 ˚C, bacterial concentration 108 CFU/mL (0.5 McFarland), and time of incubation 72 h.

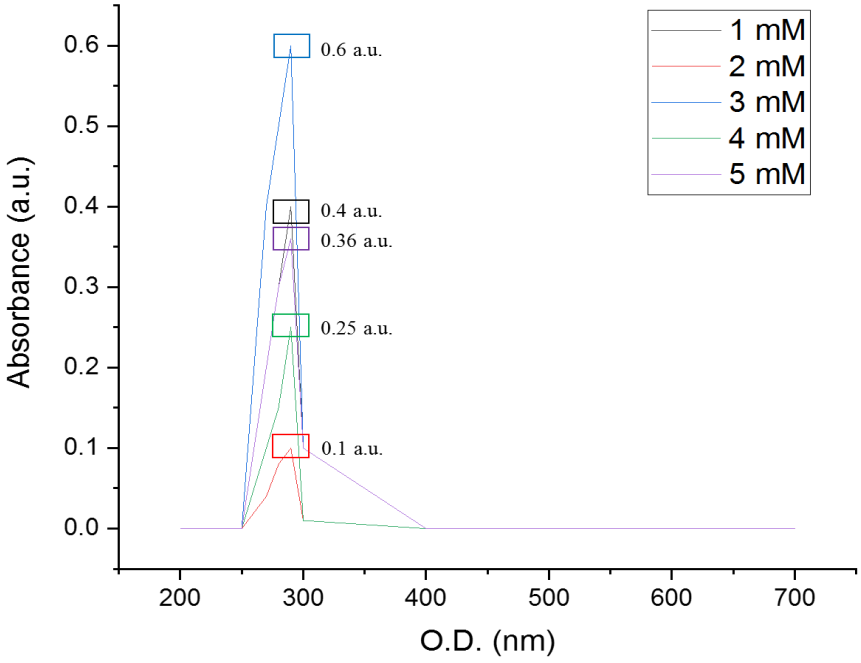

Fig.7: Absorbance peaks of the Mg NPs in the range of 200 - 700 nm synthesized under the following conditions: Temperature 37 ˚C, bacterial concentration 104 CFU/mL (< 0.5 McFarland), and time of incubation 48 h.

DOI: 10.54729/2959-331X.1107

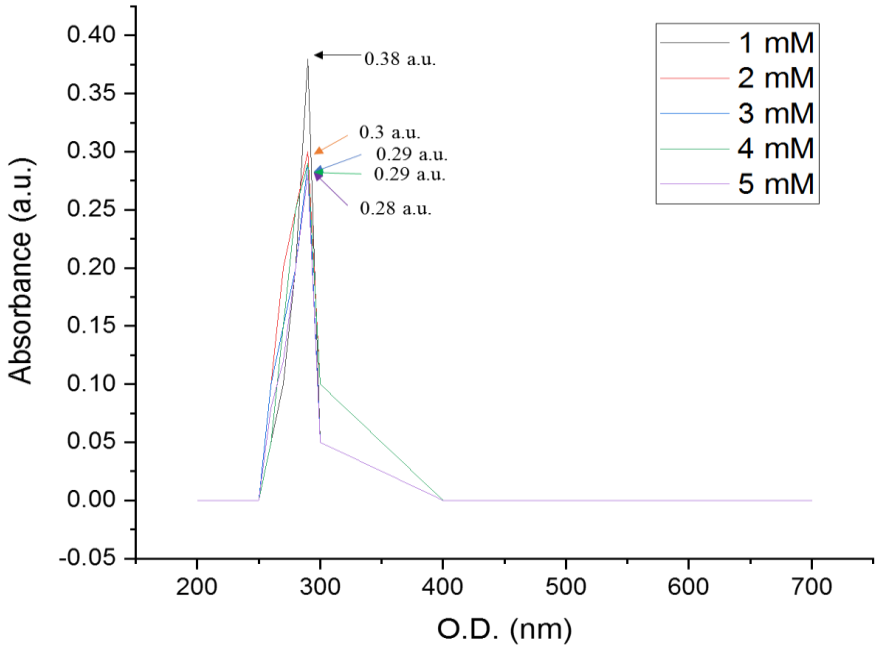

Fig.8: Absorbance peaks of the Mg NPs in the range of 200 - 700 nm synthesized under the following conditions: Temperature 37 ˚C, bacterial concentration 1012 CFU/mL (> 0.5 McFarland), and time of incubation 48 h.

3.7. FTIR Results

The FTIR analysis was performed for best sample (Mg nitrate solution of concentration 3 mM, bacterial concentration of 10^8 CFU/mL (0.5 McFarland), temperature 37 ˚C, and shaking incubation time of 48 h) (Figure 9). Various peaks were observed. A large peak was observed at 3296.09 cm^{-1}. Other peaks were observed at 2925.35 and 2957.26 cm^{-1}. Other bands were observed at 1654.47, 1543.39, and 1455.89 cm^{-1}. In addition, a band was observed at 1400.52 cm^{-1}. The capping ligands were observed at 1236.95 cm^{-1}. Another signal was observed at 1079.93 cm^{-1} The absorption peaks at 674.28 and 619.68 cm^{-1} could be attributed to O-H. The functional group of metal-oxygen bonds was given the absorption band at 568.32 and 528.58 cm^{-1}.

Fig.8: Fourier transform infrared (FTIR) spectroscopic result of the the best sample (Mg nitrate solution of concentration 3mM, bacterial concentration of 10^8 CFU/mL (0.5 McFarland), temperature 37 ˚C, and shaking incubation time of 48 h).

4. DISCUSSION

In this research, scientists created Mg NPs using the byproducts (supernatant) of a Gram-positive bacterium called *S. haemolyticus*. This bacterium was found in the wastewater of Southern Lebanese villages and is considered safe, cost-effective, and environmentally friendly (Barros et al., 2012). Certain strains of *S. haemolyticus* can produce resistant genes, which enhance their stability and help reduce metal nitrates to form metal NPs (Barros et al., 2012; Eltwisy et al., 2022). Moreover, *S. haemolyticus* is known to have a genome size of about 2 million base pairs, indicating the presence of numerous proteins that aid in reducing metal ions to create NPs (Barros et al., 2012). When the Mg nitrate solution turns from transparent to milky white, the Mg2+ ions have been reduced to Mg atoms, resulting in the creation of Mg NPs (Devi et al., 2017; Younis et al., 2021).

The UV spectra were examined within a range of 200 to 700 nm (Adnan et al., 2023; Younis et al., 2021), with the most significant peaks observed between 250 and 300 nm. The high absorbance indicates that the Mg nitrate was continuously reduced to Mg NPs. Among the samples, the highest peak was recorded at 275 nm, found in the 3 mM Mg nitrate solution. This is consistent with previous studies, such as Dolati et al.'s work on synthesizing copper oxide NPs from *Bacillus coagulans* (Dolati et al., 2023). Negative control samples did not exhibit any absorption peaks. Peaks detected before 275 nm may be attributed to amino acid residues present in the proteins extracted during the centrifugation of the bacteria. This suggests that the production of proteins during the synthesis process may be the primary factor in reducing Mg ions in the Mg nitrate solution to Mg NPs (Dolati et al., 2023; Saleh et al., 2020). These proteins can attach to the formed NPs, improving their stability.

The change in the color of the solution is explained by the release of electrons during the reduction of nitrate. This action transforms Mg^{2+} to Mg^0. The UV-Vis spectra observed within the range 250 – 300 nm are due to the excitation of the metallic free electrons during the formation of Mg nanoparticles. The absorption bands are reflected by the Mg nanoparticles due to the simultaneous vibration of the free electrons in resonance with light waves. However, the change in absorbance at different concentrations could be explained by the presence of many participating organic compounds that can interact to reduce the Mg ions. The broad absorption bands obtained suggest that the nanoparticles

were scattered without aggregation (Dolati et al., 2023; Saleh et al., 2020; Singh et al., 2020; Younis et al., 2021).

Based on the present research, it was discovered that a solution of Mg nitrate with a concentration of 3 mM produced the highest Mg NPs. The UV spectra showed a clear connection between higher concentrations of Mg nitrate solutions and increased absorbance. These results are consistent with a previous study by Saleh et al. on producing silver NPs from *K. pneumoniae* (Saleh et al., 2020)

Furthermore, there was an apparent connection between the UV spectra and the rise in *S. haemolyticus* concentration; this could be attributed to metabolite growth derived from the bacterial culture. As a result, the production of synthesized NPs increased, leading to a higher absorbance rate. This outcome is comparable to Devi et al.'s research, where they produced silver NPs from bacteria and found that increased bacterial culture concentration resulted in more NPs produced (Devi et al., 2017).

The temperature also plays an essential role in the formation of NPs. In this study, the comparison was done between the standard temperature (37 ˚C) and a higher temperature (60 ˚C). The results have shown no change in the solution color and no peaks. This means the Mg ions were not reduced and the Mg NPs were not formed. This could be because *S. haemolyticus* is a mesophilic bacterium and its metabolites cannot resist high temperatures (Barros et al., 2012; Eltwisy et al., 2022). In a prior study conducted by Saleh et al., it was discovered that silver NPs can form at a temperature of 90 ˚C (Saleh et al., 2020). However, the NPs were synthesized from *K. pneumoniae* bacterium, which is Gram-negative and known to withstand high temperatures due to its surrounding capsule (Shrivastav et al., 2013). In contrast, our *S. haemolyticus* bacteria are Gram-positive. Although they have a thick peptidoglycan layer in the cell membrane, they are more susceptible to high temperatures (Ruhal et al., 2021).

Several bacterial secondary metabolites are involved in the synthesis of metallic NPs. They aid in the reduction of metal ions to form the NPs. Among them, polysaccharides and peptides, especially chitosan and alginate, have the ability to adhere to the surface of the NPs. in addition, dextran and pullulan help in capping and stabilizing the NPs. Proteins and enzymes, including qlutathione, metallothioneins, polychelatins, oxidoreductase, cysteine desulfhydrase, and nitrate reductase play vital roles in reducing metallic ions to NPs and orienting the structure, shape, size, and morphology of the synthesized NPs (Ghosh et al., 2021).

As for the time of incubation, the best time was 48 h. Most previous studies reported that 24 h is enough to form NPs (Dolati et al., 2023; Saleh et al., 2020). All NPs synthesized from bacteria as well as green extracts are usually incubated for 24 h only. In the current study, the 24 h incubation produced Mg NPs, but the yield was smaller than that of 48 h. This revealed that the interaction between the bacterial metabolites and the Mg nitrate needed more than 24 h due to the presence of a large number of proteins in the metabolites. However, after 72 h of incubation and under the same conditions, the yield of NPs production decreased. This was illustrated by the absorbance which ranged between 0.07 and 0.5 a.u. observed between 250 – 300 nm. This means that there was no correlation between the yield and time of incubation. The decrease in the NPs' production could be explained by the oxidation of the solutions after a long incubation period (Saleh et al., 2020). This was demonstrated in several studies which focused on the agglomeration and oxidation of silver NPs as well as copper oxide NPs synthesized from bacteria and green extracts (Dolati et al., 2023; Sabouri et al., 2021; Sudarsan et al., 2021).

The mechanism of formation of the nanoparticles from bacterial metabolites is still not very clear. However, the action depends on redox reactions. Patil et al. reported that the secondary metabolites present in the bacteria are oxidized (lose electrons) and interact with the metallic ions which are reduced (gain electrons) to form metallic atoms. The reduction is followed by nucleation and eventually formation of the nanoparticles. In addition, Saleh et al. who synthesized silver (Ag) NPs from *Klebsiella pneumoniae* and tested similar conditions to this study, showed that the synthesis mechanism is enhanced by the increase in metal concentration, bacterial concentration, and temperature. However, the exact mechanism is still not very specific (Patil et al., 2017; Saleh et al., 2020).

For the FTIR results, the large peak was observed at 3296.09 cm^{-1} could be due to the OH stretching of alcohols and phenols, indicating the formation of NPs in the aqueous phase. The other peaks were observed at 2925.35 and 2957.26 cm^{-1} present the C-H stretches of methylene group of proteins and N-H group of amines. They could be due to modification in the electric environment of methyne and methylene influenced by adjacent carbon and Mg NPs. The bands observed at 1654.47, 1543.39, and 1455.89 cm^{-1} could be due to the C=C stretching vibration in the aromatic ring as well as the C=O stretching vibration in polyphenols. This suggests the presence of aldehyde, ester, or carboxylate acid group. The band observed at 1400.52 cm^{-1} could be due to the stretching modes of C–O and C–O–C. This confirms the link between Mg NPs OH / COO groups. The capping ligands which stabilize the NPs were found at 1236.95 cm^{-1}, which corresponds to the C-O-C stretch. The signal at 1079.93 cm^{-1} corresponds to the stretching of ether linkages in the flavones that are adsorbed on the surface of NPs, suggesting that the phenolic hydroxyl group is involved in the synthesis and reducing agents. The absorption peaks at 674.28 and 619.68 cm^{-1} could be attributed to O-H, where H-bonded with a broad C-O of alcohols and phenols. The functional group of metal-oxygen bonds was given the absorption band at 568.32 and 528.58 cm^{-1}, suggesting the molecular motion of Mg-O stretching (Alam et al., 2013; Dubey et al., 2017; Islam et al., 2021; Macovei et al., 2021; Wan et al., 2021).

Eventually, the best Mg NPs are synthesized by *S. haemolyticus* under the following conditions: temperature 37 ˚C, 48 h of shaking incubation, 0.5 McFarland turbidity of bacterial culture (10^8 CFU/mL), and using 3 mM of Mg nitrate solution.

5. CONCLUSION

NP synthesis has become a global phenomenon, with green synthesis outperforming physical and chemical methods. This study aimed to synthesize magnesium nanoparticles using *S. haemolyticus* under various conditions. The formation of nanoparticles was evident from the change in color of the solution, from transparent to white. The optimal Mg nitrate concentration was 3 mM, while the best bacterial concentration was the 0.5 McFarland standard (10^8 CFU/mL). After conducting tests, the optimal incubation time for Mg NP synthesis was 48 hours, and the ideal temperature was 37 ˚C. All solutions showed peaks reaching 0.9 a.u. in the 250 – 300 nm range, which confirmed the reduction of Mg ions and the formation of Mg NPs. These findings suggest that the metabolites of *S. haemolyticus* can be utilized to prepare NPs that can be applied in various domains, such as cancer treatment, antimicrobial infections, and other diseases.

REFERENCES

- Adnan, R., Abdallah, A. M., Mezher, M., Noun, M., Khalil, M., & Awad, R. (2023). Impact of Mg-doping on the structural, optical, and magnetic properties of CuO nanoparticles and their antibiofilm activity. *Physica Scripta*, *98*(5), 55935. https://doi.org/10.1088/1402-4896/acccba
- Adnan, R. M., Mezher, M., Abdallah, A. M., Awad, R., & Khalil, M. I. (2023). Synthesis, characterization, and antibacterial activity of Mg-doped CuO nanoparticles. *Molecules*, *28*(1). https://doi.org/10.3390/molecules28010103
- Alam, M., Roy, N., Mandal, D., & Begum, N. A. (2013). Green chemistry for nanochemistry: Exploring medicinal plants for the biogenic synthesis of metal NPs with fine-tuned properties. *RSC Adv.*, *3*. https://doi.org/10.1039/C3RA23133J
- Barros, E. M., Ceotto, H., Bastos, M. C. F., Dos Santos, K. R. N., & Giambiagi-Demarval, M. (2012). *Staphylococcus haemolyticus* as an important hospital pathogen and carrier of methicillin resistance genes. *Journal of Clinical Microbiology*, *50*(1), 166–168. https://doi.org/10.1128/JCM.05563-11
- Bayda, S., Adeel, M., Tuccinardi, T., Cordani, M., & Rizzolio, F. (2019). The history of nanoscience and nanotechnology: From chemical-physical applications to nanomedicine. *Molecules (Basel, Switzerland)*, *25*(1). https://doi.org/10.3390/molecules25010112
- Devanesan, S., & Alsalhi, M. S. (2021). Green synthesis of silver nanoparticles using the flower extract of abelmoschus esculentus for cytotoxicity and antimicrobial studies. *International Journal of Nanomedicine*, *16*, 3343–3356. https://doi.org/10.2147/IJN.S307676
- Devi, G. K., & Sathishkumar, K. (2017). Synthesis of gold and silver nanoparticles using *Mukia*

maderaspatna plant extract and its anticancer activity. *IET Nanobiotechnology*, *11*(2), 143–151. https://doi.org/10.1049/iet-nbt.2015.0054

- Dolati, M., Tafvizi, F., Salehipour, M., Komeili Movahed, T., & Jafari, P. (2023). Biogenic copper oxide nanoparticles from *Bacillus coagulans* induced reactive oxygen species generation and apoptotic and anti-metastatic activities in breast cancer cells. *Scientific Reports*, *13*(1), 1–19. https://doi.org/10.1038/s41598-023-30436-y
- Dubey, S., Sillanpää, M., & Varma, R. (2017). Reduction of hexavalent chromium using *Sorbaria sorbifolia* aqueous leaf extract. *Applied Sciences*, *7*, 715. https://doi.org/10.3390/app7070715
- Eltwisy, H. O., Twisy, H. O., Hafez, M. H., Sayed, I. M., & El-Mokhtar, M. A. (2022). Clinical infections, antibiotic resistance, and pathogenesis of *Staphylococcus haemolyticus*. *Microorganisms*, *10*(6). https://doi.org/10.3390/microorganisms10061130
- Feroze, N., Arshad, B., Younas, M., Afridi, M. I., Saqib, S., & Ayaz, A. (2020). Fungal mediated synthesis of silver nanoparticles and evaluation of antibacterial activity. *Microscopy Research and Technique*, *83*(1), 72–80. https://doi.org/10.1002/jemt.23390
- Ghosh, S., & Turner, R. J. (2021). Editorial: Nanomicrobiology: Emerging trends in microbial synthesis of nanomaterials and their applications. *Frontiers in Microbiology*, *12*(October), 10–12. https://doi.org/10.3389/fmicb.2021.751693
- Hamida, R. S., Ali, M. A., Alkhateeb, M. A., Alfassam, H. E., Momenah, M. A., & Bin-Meferij, M. M. (2023). Algal-derived synthesis of silver nanoparticles using the unicellular *Ulvophyte* sp. MBIC10591: Optimisation, Characterisation, and Biological Activities. *Molecules*, *28*(1). https://doi.org/10.3390/molecules28010279
- Islam, S. N., Naqvi, S. M. A., Parveen, S., & Ahmad, A. (2021). Application of mycogenic silver/silver oxide nanoparticles in electrochemical glucose sensing; alongside their catalytic and antimicrobial activity. *3 Biotech*, *11*(7), 342. https://doi.org/10.1007/s13205-021-02888-4
- luids. (2021). Qrcode_Www. *Cdc*. Retrieved from 80.%09www.ncbi.nlm.nih.gov/genome/gdv/browser/?context=gene&acc=4524.
- Macovei, I., Luca, S. V., Skalicka-Woźniak, K., Sacarescu, L., Pascariu, P., Ghilan, A., … Miron, A. (2021). Phyto-functionalized silver nanoparticles derived from conifer bark extracts and evaluation of their antimicrobial and cytogenotoxic effects. *Molecules (Basel, Switzerland)*, *27*(1). https://doi.org/10.3390/molecules27010217
- Mezher, M., El Hajj, R., & Khalil, M. (2022). Investigating the antimicrobial activity of essential oils against pathogens isolated from sewage sludge of southern Lebanese villages. *Germs*, *12*(4), 488–506. https://doi.org/10.18683/germs.2022.1355
- Nicolae-Maranciuc, A., Chicea, D., & Chicea, L. M. (2022). Ag nanoparticles for biomedical applications—ynthesis and characterization—a review. *International Journal of Molecular Sciences*, *23*(10). https://doi.org/10.3390/ijms23105778
- Patil, M. P., & Kim, G. Do. (2017). Eco-friendly approach for nanoparticles synthesis and mechanism behind antibacterial activity of silver and anticancer activity of gold nanoparticles. *Applied Microbiology and Biotechnology*, *101*(1), 79–92. https://doi.org/10.1007/s00253-016-8012-8
- Rahman, A., Kumar, S., Bafana, A., Lin, J., Dahoumane, S. A., & Je, C. (2019). Silver nanoparticles using extracellular polymeric substances of *Chlamydomonas reinhardtii*. *Molecules*, *24*, 1–19.
- Roco, M. C. (2012). National nanotechnology initiative. *Leadership in Science and Technology: A Reference Handbook*, 762–771. https://doi.org/10.4135/9781412994231.n87
- Ruhal, R., & Kataria, R. (2021). Biofilm patterns in gram-positive and gram-negative bacteria. *Microbiological Research*, *251*, 126829. https://doi.org/10.1016/j.micres.2021.126829
- Sabouri, Z., Rangrazi, A., Amiri, M. S., Khatami, M., & Darroudi, M. (2021). Green synthesis of nickel oxide nanoparticles using *Salvia hispanica* L. (chia) seeds extract and studies of their photocatalytic activity and cytotoxicity effects. *Bioprocess and Biosystems Engineering*, *44*(11), 2407–2415. https://doi.org/10.1007/s00449-021-02613-8
- Saleh, M. N., & Khoman Alwan, S. (2020). Bio-synthesis of silver nanoparticles from bacteria *Klebsiella pneumoniae*: Their characterization and antibacterial studies. *Journal of Physics: Conference Series*, *1664*(1). https://doi.org/10.1088/1742-6596/1664/1/012115
- Shrivastav, A., Lee, J., Kim, H.-Y., & Kim, Y.-R. (2013). Recent insights in the removal of *Klebseilla* pathogenicity factors for the industrial production of 2,3-butanediol. *Journal of*

Microbiology and Biotechnology, *23*(7), 885–896. https://doi.org/10.4014/jmb.1302.02066

- Singh, A., Gautam, P. K., Verma, A., Singh, V., Shivapriya, P. M., Shivalkar, S., … Samanta, S. K. (2020). Green synthesis of metallic nanoparticles as effective alternatives to treat antibiotics resistant bacterial infections: A review. *Biotechnology Reports*, *25*, e00427. https://doi.org/10.1016/j.btre.2020.e00427
- Sudarsan, S., Shankar, M. K., Motatis, A. K. B., Shankar, S., Krishnappa, D., Mohan, C. D., … Siddaiah, C. N. (2021). Green synthesis of silver nanoparticles by cytobacillus firmus isolated from the stem bark of *Terminalia arjuna* and their antimicrobial activity. *Biomolecules*, *11*(2), 1–16. https://doi.org/10.3390/biom11020259
- The different dimensions of nanotechnology. (2009). *Nature Nanotechnology*, *4*(3), 135. https://doi.org/10.1038/nnano.2009.24
- Tortorella, E., Tedesco, P., Esposito, F. P., January, G. G., Fani, R., Jaspars, M., & De Pascale, D. (2018). Antibiotics from deep-sea microorganisms: Current discoveries and perspectives. *Marine Drugs*, *16*(10), 1–16. https://doi.org/10.3390/md16100355
- Uddin, S., Safdar, L. Bin, Iqbal, J., Yaseen, T., Laila, S., Anwar, S., … Quraishi, U. M. (2021). Green synthesis of nickel oxide nanoparticles using leaf extract of *Berberis balochistanica*: Characterization, and diverse biological applications. *Microscopy Research and Technique*, *84*(9), 2004–2016. https://doi.org/10.1002/jemt.23756
- Wan, H., Li, C., Mahmud, S., & Liu, H. (2021). Kappa carrageenan reduced-stabilized colloidal silver nanoparticles for the degradation of toxic azo compounds. *Colloids and Surfaces A: Physicochemical and Engineering Aspects*, *616*, 126325. https://doi.org/https://doi.org/10.1016/j.colsurfa.2021.126325
- Younis, I. Y., El-Hawary, S. S., Eldahshan, O. A., Abdel-Aziz, M. M., & Ali, Z. Y. (2021). Green synthesis of magnesium nanoparticles mediated from *Rosa floribunda* charisma extract and its antioxidant, antiaging and antibiofilm activities. *Scientific Reports*, *11*(1), 1–15. https://doi.org/10.1038/s41598-021-96377-6
- Zia, M., Gul, S., Akhtar, J., Ul Haq, I., Abbasi, B. H., Hussain, A., … Chaudhary, M. F. (2017). Green synthesis of silver nanoparticles from grape and tomato juices and evaluation of biological activities. *IET Nanobiotechnology*, *11*(2), 193–199. https://doi.org/10.1049/iet-nbt.2015.0099